ACS Catalysis

Research Article

Cite This: ACS Catal. 2018, 8, 11794−11800

pubs.acs.org/acscatalysis

Reversible Restructuring of Silver Particles during Ethylene Epoxidation

Arno J. F. van Hoof,[†] Ivo A. W. Filot,[†] Heiner Friedrich,[‡] and Emiel J. M. Hensen*[,†]

[†]Laboratory of Inorganic Materials Chemistry, Schuit Institute of Catalysis, Eindhoven University of Technology P.O. Box 513, 5600 MB Eindhoven, The Netherlands

[‡]Laboratory of Materials and Interface Chemistry, Eindhoven University of Technology P.O. Box 513, 5600 MB Eindhoven, The Netherlands

Supporting Information

ABSTRACT: The restructuring of a silver catalyst during ethylene epoxidation under industrially relevant conditions was investigated without and with vinyl chloride (VC) promotion. During non-VC-promoted ethylene epoxidation, the silver particles grow and voids are formed at the surface and in the bulk. Electron tomography highlighted the presence of voids below the Ag surface. A mechanism is proposed involving reconstruction of the silver lattice and defect sites induced by oxygen adsorption on the external surface and grain boundaries, which finally create pores. Promotion of the catalytic reaction by VC suppresses to a significant extent void formation. The use of VC also redisperses silver particles, initially grown during ethylene epoxidation without VC. This process is rapid as the average size decreased from 172 to 136 nm within 2 h. These insights emphasize the dynamic nature of the silver particles during the ongoing ethylene epoxidation reaction and indicate that particle size and morphology strongly depend on reaction conditions.

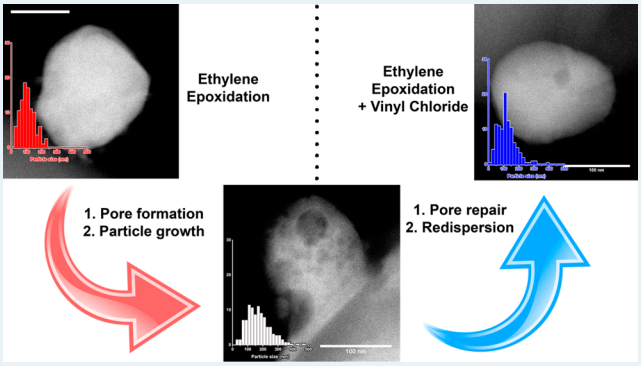

KEYWORDS: *heterogeneous catalysis, ethylene epoxidation, silver, chlorine, restructuring, redispersion, tomography*

Ethylene epoxidation toward ethylene oxide (EO) is a major chemical process with a worldwide production of ca. 34.5 × 10^6 tons of EO per year.[1] Due to its unique electronic properties, silver is regarded as the only catalyst that is sufficiently active and selective for commercial EO production.[2] Industrially, a ∼90% EO selectivity is achieved by the addition of small amounts of solid promoters to the catalyst such as Cs, Re, and Mo. In addition, a gaseous organochlorine promotor, e.g., vinyl chloride (VC), often referred to as a moderator, is cofed on-stream in ppm levels to increase the EO selectivity by modification of the active sites.[3,4] In ethylene epoxidation under industrial reaction conditions (200−250 °C, 15−20 bar), the initially metallic silver particles partially oxidize, forming a unique silver and oxygen containing surface for the catalytic reaction.[5,6] A profound influence of the chemical composition, size, and shape of nanoparticles on the catalytic performance has been demonstrated for many reactions including epoxidation reactions.[7−9] Furthermore, the impact of the catalytic reaction itself on the structure of the catalyst particles, resulting in dynamic behavior, has been emphasized.[6,10−12] This necessitates a detailed understanding of how catalytically active structures evolve under reaction conditions to establish much-sought structure-performance relations.

The restructuring of silver particles during ethylene epoxidation has been investigated in a few studies.[7,13−15] It was shown that changes in surface composition, roughness, size, and shape and the formation of holes can occur. Nevertheless, most of these findings pertain to model reaction conditions, i.e., usually atmospheric pressure is employed, and the effect of chlorine promotion has not been investigated in detail. Here, we systematically investigate the effect of chlorine, which has a profound effect on stabilizing the dispersion of silver particles during the ongoing ethylene epoxidation reaction. Without chlorine, particle restructuring occurs, resulting in voids as well as a substantial increase in particle size. For this study, we employed a procedure from the patent literature to prepare a silver epoxidation catalyst by impregnating the support material with a solution containing a silver−ethylene diamine precursor complex.[16] The silver catalyst supported on α-Al_2O_3 is tested under industrial conditions (20 bar, 225 °C) in the presence and absence of the VC promoter (Figure 1a). The silver particle morphology is investigated in dependence of time on stream using scanning transmission electron microscopy (STEM) imaging and

Received: August 20, 2018
Revised: October 30, 2018
Published: November 8, 2018

DOI: 10.1021/acscatal.8b03331
ACS Catal. 2018, 8, 11794−11800

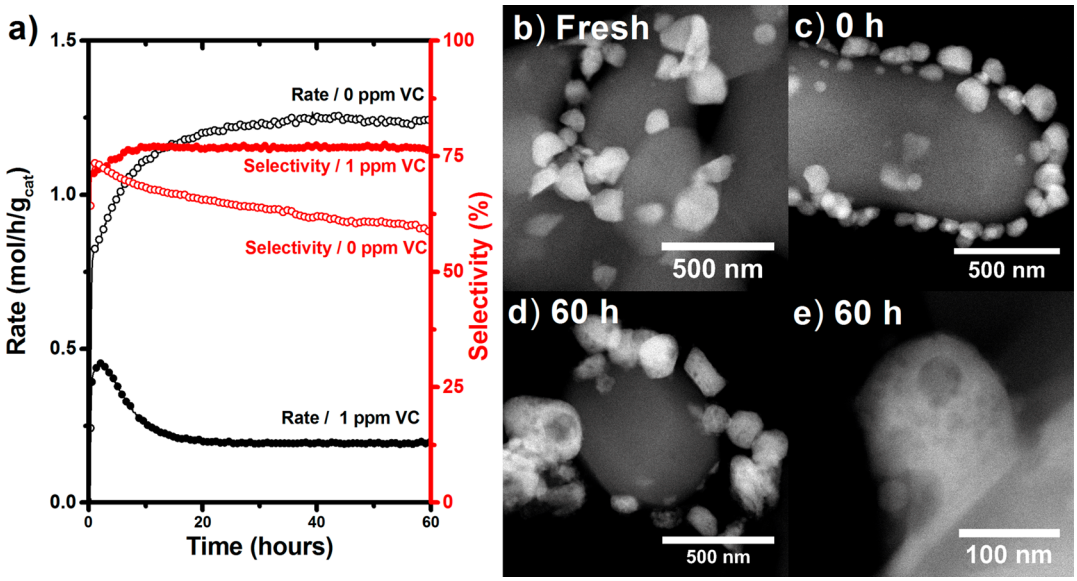

Figure 1. (a) Ag/α-Al_2O_3 reaction rate and selectivity without and with VC promotion. STEM images of (b) fresh Ag/α-Al_2O_3 catalyst, (c) Ag(0h)/α-Al_2O_3, and (d, e) Ag(60h)/α-Al_2O_3.

Table 1. STEM and X-ray Diffraction (XRD) Data for Fresh and Spent Samples[a]

sample[b]	particle size (nm)	σ (nm)	n	XRD grain size (nm)	average pore size (nm)	number of pores	porosity (%)
Ag/α-Al_2O_3	107	47	199	30			
Ag(0h)/α-Al_2O_3	119	58	250	27			
Ag(2h)/α-Al_2O_3	132	60	256	26	20	3.9	1.70
Ag(20h)/α-Al_2O_3	151	65	254	25	19	8.1	2.52
Ag(60h)/α-Al_2O_3	172	79	252	24	21	14.6	3.99
Ag(60h + 2h)/α-Al_2O_3	136	66	300				
Ag(60h + 20h)/α-Al_2O_3	127	50	300				
Ag(60h + 60h VC)/α-Al_2O_3	119	59	210	31	25	3.7	2.48
Ag(60h VC)/α-Al_2O_3	93	34	150	32	24	3.5	2.07

[a]Extended data in Table S2. [b]Detailed sample description in Table S1.

tomography. Detailed information on sample preparation, catalytic testing, and characterization is provided in the Supporting Information, section S1.

The synthesized catalyst contained a nominal weight loading of 8.2 wt % silver. The XRD pattern (Figure S1) contains peaks corresponding to metallic silver phases as well as corundum of the α-Al_2O_3 support. X-ray photoelectron spectroscopy (XPS) proved that all nitrogen from the precursor complex was completely removed (Figure S2). No evidence of bulk silver oxide was found by XRD, XPS, or electron diffraction. The average Ag particle size of the fresh catalyst, as determined by STEM analysis (Figure 1b), is 107 ± 47 nm and is comparable in size and preparation methods to industrial catalysts.[5] The crystalline domain size of the metallic silver particles is 30 nm (determined by analysis of XRD line widths). This implies that each silver particle seen in Figure 1b–e is composed of multiple domains and thus contains grain boundaries.

Before each catalytic test, a pretreatment in an oxidative environment (20 bar, 225 °C, 10% O_2 in He, 3 h) was performed. The catalytic performance was evaluated under industrial reaction conditions (20 bar, 225 °C, 5% C_2H_4, 10% O_2) for up to 60 h. In the absence of the chlorine promoter (Figure 1a), the rate slowly increases over time and stabilizes after ~20 h, while the selectivity steadily decreases to 60% after 60 h. When 1 ppm of VC is cofed, the activity reaches a maximum after 2 h, after which a fast decrease is observed. Nevertheless, with 1 ppm VC (the optimal amount for these conditions[17]), the selectivity reaches 80% after 10 h and subsequently remains constant. The decrease in the total rate has been linked to partial coverage of the catalytic surface by chlorine.[18] XPS data indeed show that, after catalysis with VC, a small amount of Cl is deposited on the catalyst surface (Figure S2). Our results are in line with previous studies and are representative for pure Ag catalysts.[18,19]

Restructuring of the initially pore-free fresh catalyst was investigated in detail by high-angle annular dark-field STEM (HAADF-STEM) imaging and electron tomography on samples that were tested in ethylene epoxidation for 0, 2, 20, and 60 h (Table S1). The 0 h sample was only pretreated without exposure to the reaction feed (Figure 1c). The average sizes and size distributions of the silver particles are listed in Table 1, and the corresponding histograms are shown in Figure S4. STEM images in Figure 1 display the fresh (Figure 1b), pretreated (Figure 1c), and 60 h on-stream samples in the absence of VC (Figure 1d and e). Using XRD, XPS, and electron diffraction, no evidence of silver oxide was found in the spent samples.

For the reaction without VC, the initial number-average particle size is 107 nm (σ = 47 nm). In situ oxidative pretreatment increased the particle size slightly to 119 nm (σ = 58 nm). When subjected to ethylene epoxidation at 225 °C,

DOI: 10.1021/acscatal.8b03331
ACS Catal. 2018, 8, 11794–11800

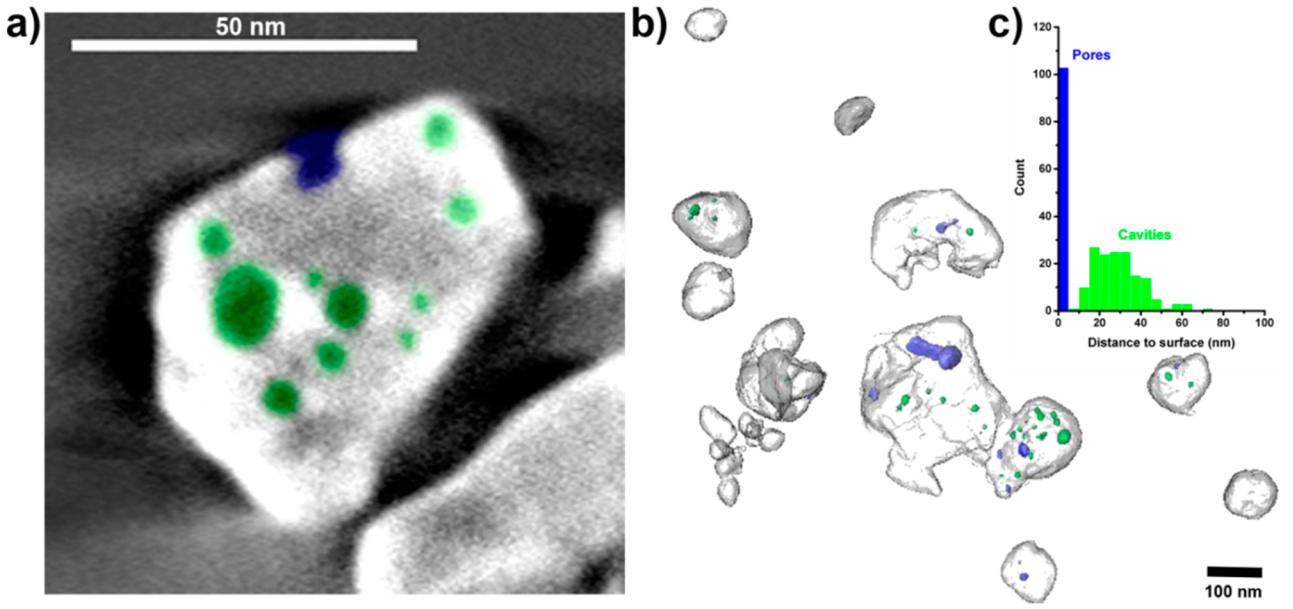

Figure 2. (a) Numerical cross section through tomogram of Ag(60h)/α-Al_2O_3. Pores are highlighted in blue, and cavities are highlighted in green. (b) Surface rendering of silver particles with pores (blue) and cavities (green). (c) Distances of cavities and pores to the external surface.

the average particle size increased to 172 nm and the particle size distribution broadened to 79 nm after 60 h. Importantly, we could establish that substantial growth of the silver particles did not occur in reference experiments in which the catalyst was exposed for 60 h to the individual reaction gases at the same pressure and temperature (Table S3).

Thus, we infer that significant particle growth is only linked to ethylene epoxidation. Growth of silver particles during epoxidation has been discussed before and is thought to occur via Ostwald ripening or coalescence.[20−22] The particle size increase results in a loss of the silver surface area, in our case of roughly 30%. Despite the loss of surface area, we observe over time a higher total reaction rate. This shows that the catalytic activity is not determined by the surface area only but that changes in the chemical surface composition and the structure play a significant role.[4,7]

Most interestingly, the STEM images (Figure 1d and e) of the 60 h spent sample show clear voids in the silver particles. Images of these samples were quantified in terms of pore size and pore frequency per silver particle (Table 1) using in-house developed software (see Supporting Information section 1 and Figure S8, for example). The average size of the voids after 60 h epoxidation reaction is 21 nm. We show in the Supporting Information (Figure S5) that void formation only occurs during epoxidation. Other possible causes such as the Kirkendall effect during the exposure to the individual gases, decomposition of silver species during quenching of the reactor, and electron beam damage have been excluded (Supporting Information section 5). As shown before, voids were not observed in the fresh sample (Figure 1b) or after oxidative pretreatment (Figure 1c). Thus, our STEM analysis shows that the ethylene epoxidation reaction leads to sintering of the silver particles and the appearance of voids.

On the other hand, XRD shows that the silver crystallite size changes only very slightly (Table 1). To get a more detailed insight into the void distribution throughout the silver particles, STEM electron tomography was employed. Numerical cross sections through silver particles are shown in Figure 2 (see also Figure S9), and a complete reconstruction is provided in the Supporting Information, Movie 1. From Figure 2, it becomes clear that the voids are located both at the external surface and in the interior of the silver particles. Voids connected to the external silver surface are termed "pores" and are marked blue in Figure 2. Voids located in the interior (without any connection to the exterior surface) are termed "cavities" and are marked green. We quantified pores and cavities in terms of location and size, including the interfacial areas between silver, α-Al_2O_3, and the vacuum (Table S4). These results show that cavities are located as deep as 60 nm below the silver surface. The observation of voids inside the silver particles clarifies that morphological changes are not restricted to the silver surface (e.g., due to an etching-like process[23]), but that the formation of cavities also occurs in the bulk. One possible explanation could be that absorbing reactant gases on the surface diffuse via the grain boundaries of the particle and initiate cavity formation. As shown with O_2 desorption (Figure S14), the oxygen capacity of the silver is well above the monolayer coverage based on the average particle size (5.3 ML). Taking into account the average crystallite size of 28 nm, we estimate that the coverage of the primary silver crystallites by O atoms is ∼1 ML. This result strongly suggests that oxygen can adsorb on the silver particles and O atoms diffuse to subsurface positions, likely along grain boundaries of the silver crystallites that make up the large silver particles.[24] That is to say, void formation started at the surface of the crystallites in the outer shell of the silver particles. This implies that the formation of the pores started before cavity formation. This hypothesis is strengthened by the observation that the pores are on average a few nm larger than the cavities and that the pores deepest into the particle are the smallest (Table S4). Another indication is that the number of voids is declining deeper into the bulk of the silver particles. All this provides a reasonable explanation for the observation that the void size is linked to the presence of crystalline domains and their grain boundaries. The diffusion of oxygen along the grain boundaries into silver particles has been observed before in silver catalysts used for the oxidation of methanol to formaldehyde.[24,25] The relation between the formation of

DOI: 10.1021/acscatal.8b03331
ACS Catal. 2018, 8, 11794−11800

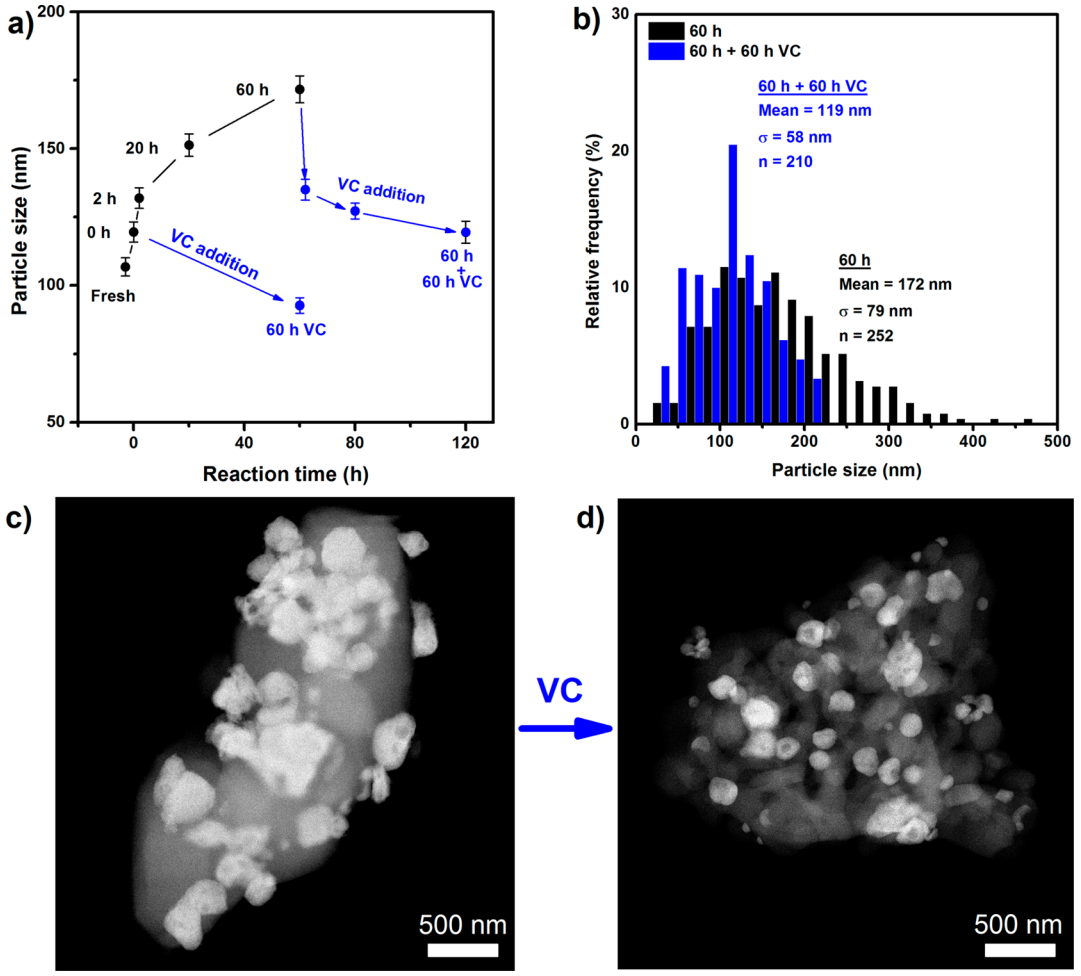

Figure 3. (a) Evolution of particle size during ethylene epoxidation and the effect of on-stream VC addition, marked in blue. Error bars in standard error of mean. (b) Particle size distribution based on STEM images for Ag(60h)/α-Al_2O_3 (black) and Ag(60h)/α-Al_2O_3 (blue). (c) STEM images of Ag(60h)/α-Al_2O_3 and (d) STEM image of Ag(60h + 60h)/α-Al_2O_3.

pores and grain boundaries is further emphasized in Figure S12. Because no Ag oxide was detected with XRD, XPS, and electron diffraction and given the fact that Ag_2O is thermodynamically unstable under reaction conditions, we suspect a role of the adsorbed oxygen layer, both on the external surface and the grain boundaries, opposed to bulk oxides in the Kirkendall effect. Oxygen adsorption can lead to the formation of defect sites (vacancies) and the rearrangement of the metal surface.[26,27] These rearrangements have been argued to cause the pore/hole formation observed for the methanol oxidation over electrolytic silver. We therefore hypothesize that repetitive cycles of oxygen adsorption and desorption, which only occur under reaction conditions, can cause the formation of stacking faults.[28,29] Accumulation of these defects and stacking faults can finally lead to the formation of the observed pores and cavities.

To understand silver particle growth in more detail, we quantified the particle size at different time-points during the ethylene epoxidation reaction, also including effects of VC promotion (Table 1 and Figure 3a and b). Representative HAADF-STEM images and histograms are reported in the Supporting Information (section S4). Table 1 contains the main results of the HAADF-STEM analysis and highlights that the porosity and number of pores gradually increases during the ongoing ethylene epoxidation reaction. The average pore size (~20 nm) and crystallite size (~25 nm) remain constant over time. This further adds evidence to the correlation between the void size and the size of the silver crystallites. Another observation is that the average pore size does not change with particle size. That is to say, only the number of pores depends on the particle size, while the average porosity remains constant (Figure S11). This implies that the average size of the pores is always smaller than the average crystalline domain size.

When the reaction is promoted by 1 ppm of VC, no significant increase of the particle size is observed after 60 h of time on stream (Table 1), indicating that Cl prevents growth of the silver particles. Notably, comparing the size of the pretreated sample with the spent sample, the silver particles even become smaller (Table 1, 0 and 60 h, and Figure 3a).

Additionally, in the presence of VC, the number of pores (and resulting porosity) is significantly lower than that without VC. A comparable behavior was observed for ethylene epoxidation reactions carried out with and without VC at different temperatures and pressures (Figure S10). While VC largely suppressed void formation, the average size of the voids was slightly larger (~24 nm) and the XRD crystallize size also increased to ~32 nm. Therefore, a correlation between the crystallites (and their grain boundaries) and the void-formation process seems plausible. One possibility, based on our data, is

DOI: 10.1021/acscatal.8b03331
ACS Catal. 2018, 8, 11794−11800

that oxygen uptake driven by continued oxidation−reduction processes creates stacking faults at the surface and grain boundaries, which then finally nucleate to the observed pores.

To investigate whether VC influences the size change and void formation dynamically, a catalyst was first exposed to the standard reaction conditions without exposure to VC for 60 h. This led to silver particle sintering (average size 172 nm) and a porosity of 4%. Then, 1 ppm VC was added to the reaction mixture and the particle size was analyzed after 2, 20, and 60 h of ethylene epoxidation. Remarkably, analysis of STEM images shows that the addition of VC led to a substantial decrease of the average particle size within 2 h to 136 nm. In the following hours the particle size further decreased to 119 nm (Figure 3a) combined with a significant narrowing of the size distribution. This effect was also observed when comparing the pretreated sample (average size 119 nm) with the spent sample only exposed to a reaction mixture containing 1 ppm VC (average size 93 nm) (Figure 3b).

These results confirm that the size increase of silver particles can be reversed by the addition of VC to the reaction feed. To support these conclusions, we ran another reaction for 60 h without VC and took out part of the catalyst for STEM analysis. The rest of the catalyst was further subjected to 60 h reaction with 1 ppm VC. The STEM analyses confirm that after reaction without VC the average particle size of 175 nm was reduced to 121 nm after further reaction with VC; both data points are within the error of measurement, emphasizing the reproducibility (Figure S15). Our results are supported by preceding studies, which found that redispersion of nanoparticles of platinum, gold, and silver by organohalides such as 1,2,-dichloropropane is possible.[30−32] Opposed to our results, the metallic nanoparticles completely redispersed via metal-halide intermediate species toward atomically isolated sites. We do not observe this full redispersion, neither when VC is added from the start nor after 60 h of reaction. Therefore, we propose that the redispersion of silver in the ethylene epoxidation follows a different mechanism. Possible explanations could be changes in the interaction of the support and changes in the (thermodynamic) stability of the silver particles that influence the wetting behavior, or breakup of the particles via grain boundaries, where also the oxidation of the silver atoms plays an important role.

Concomitant with silver redispersion, we observed that the presence of VC drastically decreased the porosity as well as the number of pores (Table 1, Ag(60h + 60h VC)), while the average void size (∼25 nm) and crystallite size (31 nm) slightly increased. These important findings show that VC is dynamically changing the bulk structure of the silver particles rather than suppressing the degree of restructuring by lowering the reaction rate. Indeed, when decreasing the reaction rate by a lower operating pressure, the same degree of pore formation is observed (Figure S10). The idea that the silver particles are a dynamically evolving system depending on the gas composition during the ethylene epoxidation reaction has been hypothesized before.[23,33,34] Our findings demonstrate that these dynamics are not limited to the catalyst surface only. Crucially, they also show that the silver particle size depends on the gas composition and that the sintering induced in a chlorine-free feed can be reversed by addition of Cl.

In summary, during the ethylene epoxidation reaction both an increase of the size of and the formation of voids in silver particles are observed as part of a dynamic restructuring process. Void formation occurs at the surface as well as in the bulk, most likely initiated close to the grain boundaries of the crystalline subdomains. The observations that the average pore size and crystallite size are relatively small and that mainly the number of pores is affected by changes in the conditions further support the idea that the voids are formed at the silver crystallite scale.

Tentatively, we propose the following mechanism. Exposure to oxygen results in oxygen adsorption on the silver surface and dissolution of oxygen atoms in the bulk, likely also via diffusion and adsorption along the grain boundaries between the primary crystallites that make up the silver particles. At this stage, no voids are formed as observed for the freshly activated sample and a sample held at reaction conditions in oxygen for 60 h. Addition of ethylene to the gas feed results in partial reduction of the surface, resulting in the formation of ethylene oxide. We speculate that a part of the oxygen dissolved in the bulk will migrate to the external surface, while at the same time oxygen is being replenished by diffusion along grain boundaries. The repeating adsorption of oxygen on the grain boundaries might then lead to stacking faults and nucleation of voids within a crystallite.

The role of the pores on the epoxidation reaction is difficult to assess, because the additional external surface created by the pores contributes <2% to the overall external Ag surface area (Table S4). Besides extra external surface, the formed pores could also be beneficial for overall reaction rate, as they can increase oxygen diffusion into the bulk.[29] Additionally, the presence of these pores and cavities is a strong indication that not only the external surface area of the silver particle is affected by catalysis but almost the complete particle is involved. The structural dynamics are therefore multifaceted and may also influence the sintering and redispersion aspects noted in this Article. The role of chlorine is mainly to suppress the unwanted complete oxidation of ethylene.[3,4] Chlorine also covers the surface, so that the total reactivity is significantly suppressed. Given our observations that chlorine also redisperses silver particles, we must take into account the fact that highly mobile species can be formed, such as AgCl species. The high mobility is in line with the low Tammann temperature of AgCl. Nevertheless, XPS data showed the presence of minor amounts of Cl in the spent samples, which could potentially influence the catalyst surface energies. The decrease of the particle size is likely due to the lower surface tension of chlorine-terminated silver particles than that of oxygen-terminated silver particles. To conclude, we have shown in this work that the ethylene epoxidation reaction affects the entire silver particle structure, not only the particle surface but also bulk regions. This is very different from traditional heterogeneous metal catalysis in which single-crystalline nanoparticles mainly feature surface effects. Our results demonstrate that silver particle size and morphology evolve dynamically and reversibly as a function of the reaction conditions. While sintering is evident during ethylene epoxidation, addition of chlorine results in smaller particles through a chlorine-induced redispersion mechanism. These insights add further support to the view that the active phase in heterogeneous catalysts is strongly dependent on the reaction conditions.

■ ASSOCIATED CONTENT

Supporting Information

The Supporting Information is available free of charge on the ACS Publications website at DOI: 10.1021/acscatal.8b03331.

DOI: 10.1021/acscatal.8b03331
ACS Catal. 2018, 8, 11794−11800

Experimental procedures; XRD; XPS; additional STEM images and size distribution; cryogenic quenching of catalyst and low-dose STEM; quantitative analysis; detailed tomography and STEM quantification data; HAADF-STEM and TEM of crystalline domain and pores; distance map; O_2-TPD; Duplo experiment; and Kolmogorov−Smirnov test (PDF)

Electron tomography reconstruction and rendering of data set 1 (MPG)

Electron tomography rendering of data set 2 (MPG)

AUTHOR INFORMATION

Corresponding Author

*E-mail: e.j.m.hensen@tue.nl.

ORCID

Arno J. F. van Hoof: 0000-0002-9649-031X

Heiner Friedrich: 0000-0003-4582-0064

Emiel J. M. Hensen: 0000-0002-9754-2417

Notes

The authors declare no competing financial interest.

ACKNOWLEDGMENTS

The authors thank the Impuls program of the Eindhoven University of Technology and a Top grant of The Netherlands Organization for Scientific Research (NWO) for funding. L. S. van Hazendonk is acknowledged for the analysis of the tomography data.

REFERENCES

(1) TechNavio. *Global Ethylene Oxide and Ethylene Glycol Market 2016−2020*; TechNavio: London, U.K., 2016.

(2) Ozbek, M. O.; Onal, I.; Van Santen, R. A. Why Silver Is the Unique Catalyst for Ethylene Epoxidation. *J. Catal.* **2011**, *284*, 230−235.

(3) Ozbek, M. O.; Onal, I.; Van Santen, R. A. Ethylene Epoxidation Catalyzed by Chlorine-Promoted Silver Oxide. *J. Phys.: Condens. Matter* **2011**, *23*, 404202.

(4) Rocha, T. C. R.; Hävecker, M.; Knop-Gericke, A.; Schlögl, R. Promoters in Heterogeneous Catalysis: The Role of Cl on Ethylene Epoxidation over Ag. *J. Catal.* **2014**, *312*, 12−16.

(5) Rebsdat, S.; Mayer, D. Ethylene Oxide. In *Ullmann's Encyclopedia of Industrial Chemistry*; Wiley-VCH Verlag GmbH & Co. KGaA: Weinheim, Germany, 2012; pp 547−572.

(6) García-Mota, M.; Rieger, M.; Reuter, K. Ab Initio Prediction of the Equilibrium Shape of Supported Ag Nanoparticles on α-Al_2O_3(0 0 0 1). *J. Catal.* **2015**, *321*, 1−6.

(7) Christopher, P.; Linic, S. Shape- and Size-Specific Chemistry of Ag Nanostructures in Catalytic Ethylene Epoxidation. *ChemCatChem* **2010**, *2*, 78−83.

(8) Christopher, P.; Linic, S. Engineering Selectivity in Heterogeneous Catalysis: Ag Nanowires as Selective Ethylene Epoxidation Catalysts. *J. Am. Chem. Soc.* **2008**, *130*, 11264−11265.

(9) Sangaru, S. S.; Zhu, H.; Rosenfeld, D. C.; Samal, A. K.; Anjum, D.; Basset, J.-M. Surface Composition of Silver Nanocubes and Their Influence on Morphological Stabilization and Catalytic Performance in Ethylene Epoxidation. *ACS Appl. Mater. Interfaces* **2015**, *7*, 28576−28584.

(10) Vendelbo, S. B.; Elkjær, C. F.; Falsig, H.; Puspitasari, I.; Dona, P.; Mele, L.; Morana, B.; Nelissen, B. J.; van Rijn, R.; Creemer, J. F.; Kooyman, P. J.; Helveg, S. Visualization of Oscillatory Behaviour of Pt Nanoparticles Catalysing CO Oxidation. *Nat. Mater.* **2014**, *13*, 884−890.

(11) Hansen, P. L.; Wagner, J. B.; Helveg, S.; Rostrup-Nielsen, J. R.; Clausen, B. S.; Topsoe, H. Atomic Resolved Imaging of Dynamic Shape Changes in Supported Copper Nanocrystals. *Science* **2002**, *295*, 2053−2055.

(12) Nolte, P.; Stierle, A.; Jin-Phillipp, N. Y.; Kasper, N.; Schulli, T. U.; Dosch, H. Shape Changes of Supported Rh Nanoparticles during Oxidation and Reduction Cycles. *Science* **2008**, *321*, 1654−1658.

(13) Wodiunig, S.; Keel, J. M.; Wilson, T. S. E.; Zemichael, F. W.; Lambert, R. M. AFM and XPS Study of the Sintering of Realistic Ag/{0001}α-Al2O3model Catalysts under Conditions of Ethene Epoxidation. *Catal. Lett.* **2003**, *87*, 1−5.

(14) Greiner, M. T.; Jones, T. E.; Johnson, B. E.; Rocha, T. C. R.; Wang, Z. J.; Armbrüster, M.; Willinger, M.; Knop-Gericke, A.; Schlögl, R. The Oxidation of Copper Catalysts during Ethylene Epoxidation. *Phys. Chem. Chem. Phys.* **2015**, *17*, 25073−25089.

(15) Dellamorte, J. C.; Lauterbach, J.; Barteau, M. A. Promoter-Induced Morphological Changes of Ag Catalysts for Ethylene Epoxidation. *Ind. Eng. Chem. Res.* **2009**, *48*, 5943−5953.

(16) Kemp, R. A.; Evans, W. E.; Matusz, M. Process for Preparing Ethylene Oxide Catalysts. EP0716884A2, 1995.

(17) Harris, J. W.; Bhan, A. Moderation of Chlorine Coverage and Ethylene Epoxidation Kinetics via Ethane Oxychlorination over Promoted Ag/α-Al2O3. *J. Catal.* **2018**, *367*, 62−71.

(18) Jankowiak, J. T.; Barteau, M. A. Ethylene Epoxidation over Silver and Copper-Silver Bimetallic Catalysts: I. Kinetics and Selectivity. *J. Catal.* **2005**, *236*, 366−378.

(19) Lee, J. K.; Verykios, X. E.; Pitchai, R. Support and Crystallite Size Effects in Ethylene Oxidation Catalysis. *Appl. Catal.* **1989**, *50*, 171−188.

(20) Hoflund, G. B.; Minahan, D. M. Study of Cs-Promoted, α-Alumina-Supported Silver, Ethylene-Epoxidation Catalysts. *J. Catal.* **1996**, *162*, 48−53.

(21) Zhou, X. G.; Yuan, W. K. Modeling Silver Catalyst Sintering and Epoxidation Selectivity Evolution in Ethylene Oxidation. *Chem. Eng. Sci.* **2004**, *59*, 1723−1731.

(22) Boskovic, G.; Wolf, D.; Brückner, A.; Baerns, M. Deactivation of a Commercial Catalyst in the Epoxidation of Ethylene to Ethylene Oxide - Basis for Accelerated Testing. *J. Catal.* **2004**, *224*, 187−196.

(23) Heine, C.; Eren, B.; Lechner, B. A. J.; Salmeron, M. A Study of the O/Ag(111) System with Scanning Tunneling Microscopy and X-ray Photoelectron Spectroscopy at Ambient Pressures. *Surf. Sci.* **2016**, *652*, 51−57.

(24) Nagy, A.; Mestl, G.; Rühle, T.; Weinberg, G.; Schlögl, R. The Dynamic Restructuring of Electrolytic Silver during the Formaldehyde Synthesis Reaction. *J. Catal.* **1998**, *179*, 548−559.

(25) Bao, X.; Lehmpfuhl, G.; Weinberg, G.; Schlogl, R.; Ertl, G. Variation of the Morphology of Silver Surfaces by Thermal and Catalytic Etching. *J. Chem. Soc., Faraday Trans.* **1992**, *88*, 865−872.

(26) Li, W. X.; Stampfl, C.; Scheffler, M. Oxygen Adsorption on Ag(111): A Density-Functional Theory Investigation. *Phys. Rev. B: Condens. Matter Mater. Phys.* **2002**, *65*, No. 075407.

(27) Jones, T. E.; Rocha, T. C. R.; Knop-Gericke, A.; Stampfl, C.; Schlögl, R.; Piccinin, S. Adsorbate Induced Vacancy Formation on Silver Surfaces. *Phys. Chem. Chem. Phys.* **2014**, *16*, 9002−9014.

(28) Waterhouse, G. I. N.; Bowmaker, G. A.; Metson, J. B. Oxygen Chemisorption on an Electrolytic Silver Catalyst: A Combined TPD and Raman Spectroscopic Study. *Appl. Surf. Sci.* **2003**, *214*, 36−51.

(29) Waterhouse, G. I. N.; Bowmaker, G. A.; Metson, J. B. Mechanism and Active Sites for the Partial Oxidation of Methanol to Formaldehyde over an Electrolytic Silver Catalyst. *Appl. Catal., A* **2004**, *265*, 85−101.

(30) Morgan, K.; Goguet, A.; Hardacre, C. Metal Redispersion Strategies for Recycling of Supported Metal Catalysts: A Perspective. *ACS Catal.* **2015**, *5*, 3430−3445.

(31) Goguet, A.; Hardacre, C.; Harvey, I.; Narasimharao, K.; Saih, Y.; Sa, J. Increased Dispersion of Supported Gold during Methanol Carbonylation Conditions. *J. Am. Chem. Soc.* **2009**, *131*, 6973−6975.

(32) Sá, J.; Goguet, A.; Taylor, S. F. R.; Tiruvalam, R.; Kiely, C. J.; Nachtegaal, M.; Hutchings, G. J.; Hardacre, C. Influence of Methyl Halide Treatment on Gold Nanoparticles Supported on Activated Carbon. *Angew. Chem., Int. Ed.* **2011**, *50*, 8912−8916.

DOI: 10.1021/acscatal.8b03331
ACS Catal. 2018, 8, 11794−11800

(33) Serafin, J. G.; Liu, A. C.; Seyedmonir, S. R. Surface Science and the Silver-Catalyzed Epoxidation of Ethylene: An Industrial Perspective. *J. Mol. Catal. A: Chem.* **1998**, *131*, 157−168.
(34) Jones, T. E.; Wyrwich, R.; Bocklein, S.; Rocha, T. C. R.; Carbonio, E. A.; Knop-Gericke, A.; Schlogl, R.; Gunther, S.; Wintterlin, J.; Piccinin, S. Oxidation of Ethylene on Oxygen Reconstructed Silver Surfaces. *J. Phys. Chem. C* **2016**, *120*, 28630−28638.

DOI: 10.1021/acscatal.8b03331
ACS Catal. 2018, 8, 11794−11800